NASA/TM–2013-218053

Notched Strength Allowables and Inplane Shear Strength of AS4/VRM-34 Textile Laminates

Ray W. Grenoble
Langley Research Center, Hampton, Virginia

William M. Johnston
Science and Technology Corporation, Hampton, Virginia

October 2013

NASA STI Program . . . in Profile

Since its founding, NASA has been dedicated to the advancement of aeronautics and space science. The NASA scientific and technical information (STI) program plays a key part in helping NASA maintain this important role.

The NASA STI program operates under the auspices of the Agency Chief Information Officer. It collects, organizes, provides for archiving, and disseminates NASA's STI. The NASA STI program provides access to the NASA Aeronautics and Space Database and its public interface, the NASA Technical Report Server, thus providing one of the largest collections of aeronautical and space science STI in the world. Results are published in both non-NASA channels and by NASA in the NASA STI Report Series, which includes the following report types:

- TECHNICAL PUBLICATION. Reports of completed research or a major significant phase of research that present the results of NASA Programs and include extensive data or theoretical analysis. Includes compilations of significant scientific and technical data and information deemed to be of continuing reference value. NASA counterpart of peer-reviewed formal professional papers, but having less stringent limitations on manuscript length and extent of graphic presentations.

- TECHNICAL MEMORANDUM. Scientific and technical findings that are preliminary or of specialized interest, e.g., quick release reports, working papers, and bibliographies that contain minimal annotation. Does not contain extensive analysis.

- CONTRACTOR REPORT. Scientific and technical findings by NASA-sponsored contractors and grantees.

- CONFERENCE PUBLICATION. Collected papers from scientific and technical conferences, symposia, seminars, or other meetings sponsored or co-sponsored by NASA.

- SPECIAL PUBLICATION. Scientific, technical, or historical information from NASA programs, projects, and missions, often concerned with subjects having substantial public interest.

- TECHNICAL TRANSLATION. English-language translations of foreign scientific and technical material pertinent to NASA's mission.

Specialized services also include organizing and publishing research results, distributing specialized research announcements and feeds, providing information desk and personal search support, and enabling data exchange services.

For more information about the NASA STI program, see the following:

- Access the NASA STI program home page at *http://www.sti.nasa.gov*

- E-mail your question to help@sti.nasa.gov

- Fax your question to the NASA STI Information Desk at 443-757-5803

- Phone the NASA STI Information Desk at 443-757-5802

- Write to:
  STI Information Desk
  NASA Center for AeroSpace Information
  7115 Standard Drive
  Hanover, MD 21076-1320

NASA/TM–2013-218053

Notched Strength Allowables and Inplane Shear Strength of AS4/VRM-34 Textile Laminates

Ray W. Grenoble
Langley Research Center, Hampton, Virginia

William M. Johnston
Science and Technology Corporation, Hampton, Virginia

National Aeronautics and
Space Administration

Langley Research Center
Hampton, Virginia 23681-2199

October 2013

Available from:

NASA Center for AeroSpace Information
7115 Standard Drive
Hanover, MD 21076-1320
443-757-5802

Abstract

Notched and unnotched strength allowables were developed for a textile composite to provide input data to analytical structural models based on the Pultruded Rod Stiffened Efficient Unitized Structure (PRSEUS) concept. Filled-hole tensile strength, filled-hole compressive strength, and inplane shear strength along stitch lines have been measured. The material system evaluated in this study is based on warp-knitted preforms of AS4 carbon fibers and VRM-34 epoxy resin, which have been processed via resin infusion and oven curing. All specimens were tested in as-fabricated (dry) condition. Filled-hole strengths were evaluated with and without through-thickness stitching. The effects of scaling on filled-hole tensile strength were evaluated by testing specimens in two widths, but with identical width / hole-diameter ratios. Inplane shear specimens were stitched in two configurations, and two specimen thicknesses were tested for each stitch configuration.

Introduction

The Pultruded Rod Stiffened Efficient Unitized Structure (PRSEUS)[1,2] concept was developed through collaborative work between NASA and Boeing on the Hybrid Wing Body (HWB). The HWB is a concept for a future airliner, based on a flying wing configuration. The width of the body center section creates a pressurized cabin with a rectangular cross-sectional shape. Whereas the elliptical shape of a conventional fuselage carries most internal pressure-driven loads through skin tension, the flat sides of the HWB pressure cabin will carry those loads primarily via bending of the cabin skin.

PRSEUS leverages lessons learned in previous NASA-sponsored textile composites development activities such as the Advanced Composites Technology (ACT) program[3,4]. ACT focused on advancing the development of carbon fiber textile-based composites. Key technology focus areas were through-thickness stitching to increase damage tolerance and the use of innovative processing methods to reduce fabrication costs. The program culminated with the fabrication (using a resin film infusion process) and testing of a representative wing box structural component with embedded impact damage.

The primary features distinguishing PRSEUS from conventional composite stiffened skin construction are:

- skins and stiffening members composed of warp-knitted, dry carbon fiber preforms
- foam-cored frames covered in a textile preforms
- stringers incorporating a precured, unidirectional carbon/epoxy rod in the outstanding flange
- through-thickness stitching between the stringer/frame lower flanges and the skin
- use of low-cost foam tooling for preform assembly
- out-of-autoclave processing (via a vacuum-assisted resin infusion process) and oven cure.

The unidirectional rod in the stringer flanges provides the structure with very high bending stiffness in the longitudinal direction. This attribute makes the concept attractive for application to HWB's pressurized cabin. The stitching at the stiffener/skin bondline is intended to suppress delamination of that critical interface well into a post-buckling loading regime[5]. It also plays a critical role in stabilizing the dry preform prior to infusion and curing of the part.

A sketch illustrating the construction of a PRSEUS structural element is shown in Figure 1. During the fabrication process, dry stiffener and frame preforms are assembled upside-down in foam/plastic tooling. The tear straps and skins are placed over the stiffening elements an
d the constituents are then stitched together through the thickness from what will be the outer mold line (OML) of the part. The position of the precured rods in the stringers relative to the skin is established by the holes through the foam cores of the frames. Once the stitched assembly is removed from the tooling, it is effectively self-supporting. This attribute greatly reduces the tooling required during the remainder of the manufacturing process. Note the presence of two lines of single stitches along the length of the stringer webs in Figure 1. The upper line forms a pocket for the pultruded rod that serves as the stringer flange. The lower line defines the bottom of the stringer web.

In PRSEUS structure, the stitches between the skins and stiffeners are placed in pairs. Figure 2 illustrates the stitch placement on a typical stringer. The first stitch enters the skin outer surface and emerges on the inner surface (bag side) near the center of the stiffening element lower flange half. This stitch is oriented normal to the skin surface. A second, inclined stitch is placed on the outer surface directly under the stiffener web. This stitch emerges on the inner surface of the structure adjacent to the stiffener web.

To date, little notched strength data for PRSEUS structure have been available in the open literature. This lack of data has prevented development of accurate analytical models of this structural concept, and has limited the ability of others outside NASA and Boeing to evaluate the suitability of the PRSEUS concept for their own applications. The present study is intended to address this deficiency by developing a set of notched strength properties for use as input to analytical models. Coupons are tested to provide data on the inplane shear, notched tensile and notched compressive strengths of PRSEUS skin for one commonly used preform type.

Materials

This study evaluates the mechanical properties of laminates fabricated from non-woven, warp-knitted preforms. The preforms were composed of seven-layers of AS4* fiber in a balanced, symmetric layup. The preform stacking sequence was [+45/-45/0/90/0/-45/+45]. Total preform thickness was 0.052 in. Fiber areal weights in each layer were scaled to attain a layup with percentages of (45/43/12) in the (0°/±45°/90°) directions, respectively. Panels were fabricated by infusing the preforms with VRM-34* epoxy resin. All filled-hole strength specimens were cut from panels made from four preforms. Inplane shear specimens were cut from panels containing either three or four preforms. Boeing Research and Technology (Huntington Beach, CA.) fabricated the panels and shipped them to NASA Langley Research Center. Ultrasonic evaluation of the delivered panels found no indications of damage or poor consolidation quality within the panels.

Some panels incorporated through-thickness stitching to represent the stitched bondline between the skins and stiffeners. Stitches were formed from 1600 denier Vectran thread. Stitch linear density was 5.08 stitches per inch. Placement of stitches followed a pattern similar to that shown in Figure 2. The stitches were placed in pairs; one stitch was oriented normal to the skin surface and one was inclined at a 56° angle relative to the tool surface. All stitch lines were oriented along specimen lengths.

Characterization

The scope of the test matrix is shown in Table 1. Each specimen set was composed of six replicates. All specimens were tested in servo-hydraulic test stands, which were fitted with hydraulic wedge grips. Filled-hole tension and compression specimens were tested in accordance with ASTM D6742. However, open-hole compression specimens required use of a support fixture, meeting the requirements for open-hole compression testing in ASTM D6484-09, to prevent buckling failure. Inplane shear specimens were tested in a fixture meeting the requirements of ASTM D7078-05. All data analysis was performed in the manner recommended by the relevant ASTM test standards.

* product of the Hexcel Corporation

Table 1. Test matrix

Test Type	ASTM Standard	Stitching†	Specimen Geometry, in	Replicates per Set
Filled-Hole Tension	D 6742	S, US	12 x 1.5 x 0.208	12
		S, US	12 x 3.0 x 0.208	12
Filled-Hole Compression	D 6742	S, US	12 x 1.5 x 0.208	12
Inplane Shear	D 7078	SA	2.2 x 3.0 x 0.157	12
		ST	2.2 x 3.0 x 0.208	12

† S = Stitched, US = UnStitched, SA = Stitched Around root of notch, ST = Stitched Through root of notch

Specimen Preparation

Filled-Hole Tension (FHT) specimens were tested in two widths, 1.5 in. and 3.0 in. The 1.5-in. wide specimens contained a single line of stitch pairs. Their stitch pattern is shown in Figure 3 The 3.0-in. wide specimens had two lines of stitches. The lines were symmetric about the specimen centerline, with normal-direction stitches positioned along the specimen edges. Details of the stitching in the 3.0-in. specimens are shown in Figure 4. All FHT specimens were approximately 0.21 in. thick, which resulted in hole diameter / specimen thickness ratios of 1.19:1 and 2.38:1 for the 1.5-in. and 3.0-in. wide specimens, respectively. Grade-8 bolts of 0.25 in. nominal diameter were used in the 1.5-in. specimens and 0.5-in. diameter bolts were used in the 3-in. wide specimens. In all FHT specimens, the nuts were tightened finger-tight. Care was taken to assure that the unthreaded shank of the bolt extended past the specimen surface. Washers were used under both the bolt head and nut.

Filled Hole Compression (FHC) specimens were 1.5 in. wide, and they incorporated a stitch pattern identical to that used in the 1.5-in. wide FHT specimens. Similar to the FHT specimens, washers were used under both the bolt head and nut and care was exercised to assure that the unthreaded shank of the bolt bore against the inside diameter of the hole. Unlike the FHT specimens, bolts through the FHC specimens were torqued to 60 lbf-in

Shear strains within the gage section of the V-Notch rail Shear (VNS) shear specimens were monitored with back-to-back strain gages mounted at ± 45° directions. The effects of stitching on shear properties were assessed by cutting VNS specimens in two configurations relative to the stitch lines. The first configuration placed the line of normal-direction stitches through the center of the notch, as seen in Figure 5(a), to concentrate shear stress on that line of stitches. The second configuration centered the notch between the two stitch lines on the inside mold line (IML) side of the panel, as shown in Figure 5(b), to focus shear stress on an area of the coupon that is not stitched.

All specimens were cut from their precursor panels by a waterjet, with the 0° laminate direction was aligned with the loading direction of each specimen type. All filled-hole specimens were drilled through the center of the gage section with diamond-grit core drills. All 1.5-in. wide specimens were drilled with 0.25-in. nominal diameter holes, and all 3.0-in. wide specimens received 0.5-in. nominal diameter holes. Consequently, all filled-hole coupons had a width / hole diameter ratio of approximately 6:1. Measured diameters of bolt holes and bolts are tabulated for each filled-hole specimen in Table A1 in the Appendix. The VNS specimens required geometric tolerances in the gage region that could not be maintained by the waterjet cutter. The final geometry of the notch on these specimens was established with a diamond grit endmill in a milling machine.

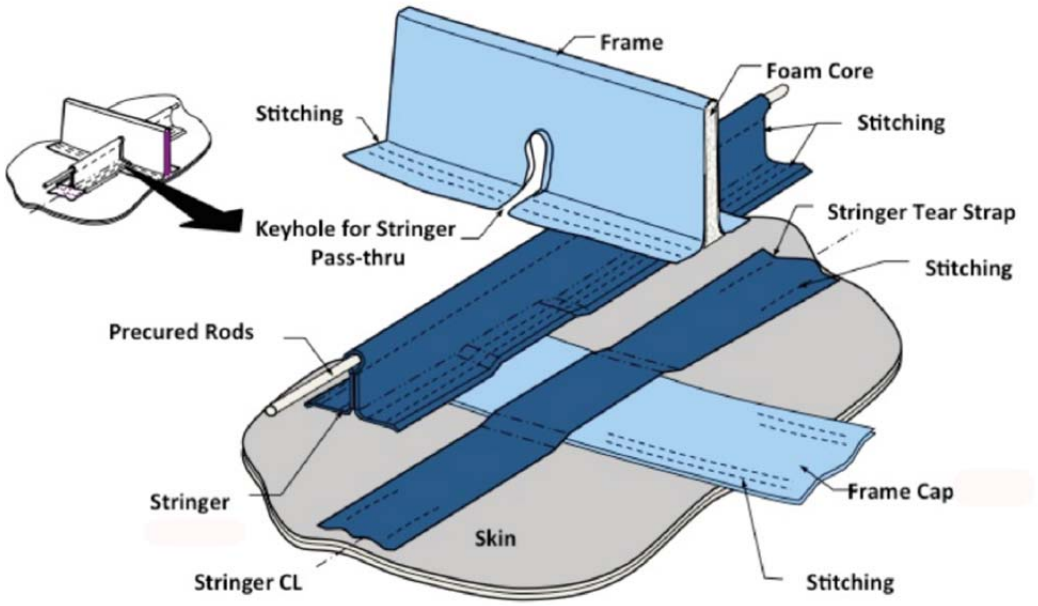

Figure 1. PRSEUS structure stringer-frame intersection, typical construction

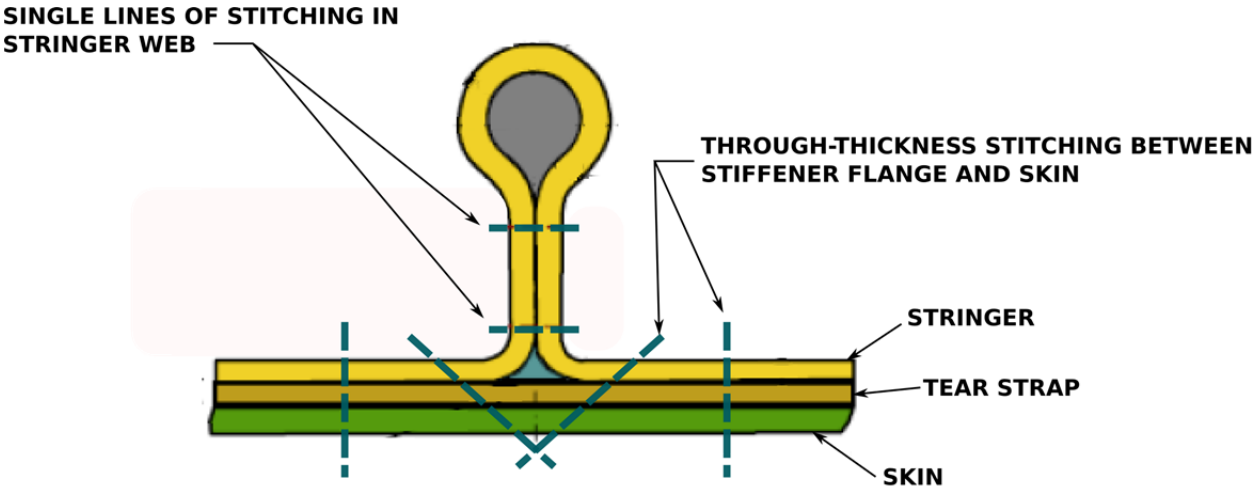

Figure 2. Cross-sectional view of stitching through typical PRSEUS skin, tear strap, and stringer.

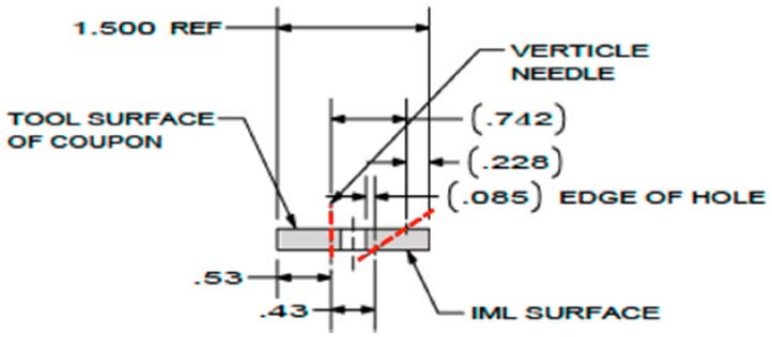

Figure 3. Stitching location on filled hole tension and filled hole compression specimens, 1.5 in. specimen width, section through center of bolt hole is shown

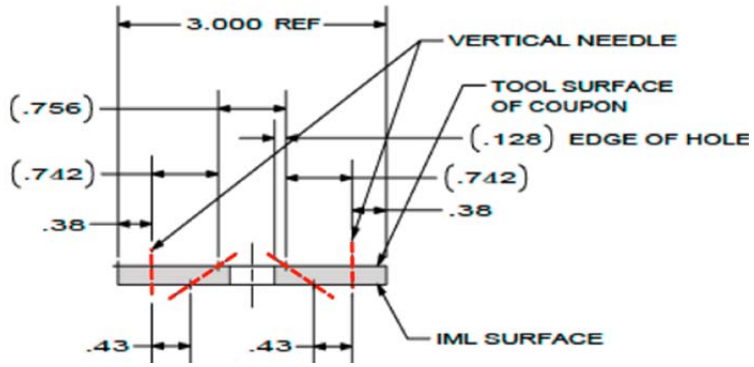

Figure 4. Stitching location on filled hole tension and filled hole compression specimens, 3.0 in. specimen width, section through center of bolt hole is shown.

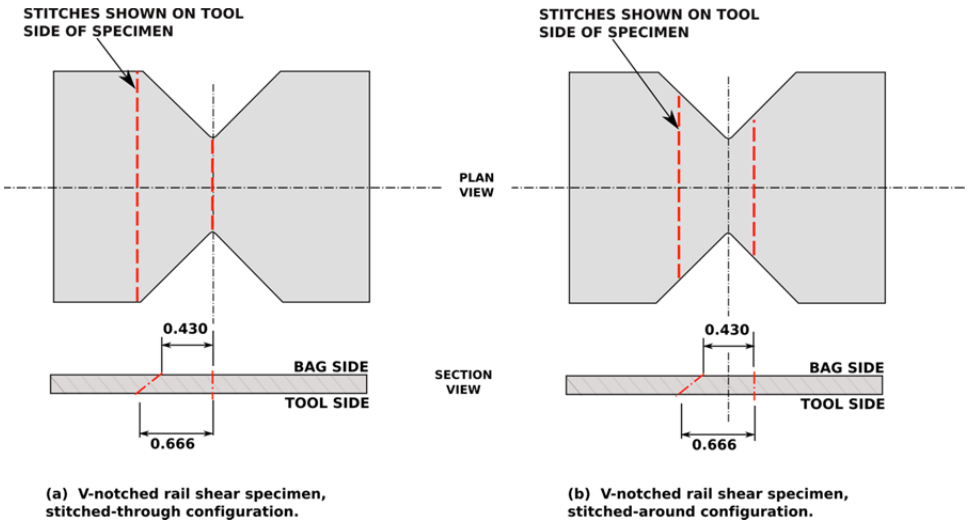

Figure 5. Stitching location shear specimens relative to the root of the notch.

Results

In this section, a discussion of test results is provided, followed by the tabulated results. Values for gross section strength and net section strength are provided for the filled-hole specimens. Gross section strength neglects the presence of the bolt hole; whereas net section strength accounts for the presence of the hole. Supplemental information to the measured strength data is provided in the Appendix. As-tested bolt and hole diameters for filled-hole specimens are provided in Table A1. Observed failure modes of individual filled-hole specimens are compiled in Tables A2 through A4. Post-test photographs of test specimens are also included in the Appendix; Figures A1 and A2 show the four sets of FHT specimens, Figure A3 shows the two sets of FHC specimens, and Figures A4 and A5 show the four VNS specimen sets.

The results of filled-hole tension testing are tabulated in Table 2. Examination of Table 2(a) shows that the stitching had no detrimental effect on the filled-hole tensile strength of the 1.5-inch wide specimens. The average ultimate strength was higher and the degree of variability in the strength of the stitched specimens was lower than that of the unstitched specimens. Looking at section (b) of Table 2, it is evident that the average strength of the 3-in. wide stitched specimens was two standard deviations (2σ) higher than the strength of the unstitched specimens. However, the amount of variability in the strength increased as well. Overall, the increase in specimen width from 1.5 in. to 3.0 in. resulted in a decrease in apparent filled-hole tensile strength. The strength of unstitched specimens decreased by 16%, and the strength of stitched specimens decreased by 10% when the specimen width doubled. Some of this decrease in strength may be attributed to the condition of the bolt holes in those specimens. Table A1 shows that the bolt hole clearance in both sets of 3-in. wide specimens averaged approximately 0.016 in. A clearance of approximately 0.003 in. was expected, based on the tools used to drill the holes and the fasteners used. An unexpected amount of variation in the hole diameters is also evident. Based on those observations, the presence of non-visible damage in the bolt holes cannot be ruled out. The source of the discrepancies in hole diameter has not been identified. In both specimen sets, the stitching appears to have constrained the propagation of delaminations. Examination of Figure A1(b) reveals that delamination of the 1.5-in. stitched specimen was most severe along the edges, outside the stitch lines. The 3.0-in. wide FHT specimens displayed a greater degree of surface ply delamination than did the 1.5-in. specimens, which is clearly seen in Figure A2(b). Delamination in the 3.0-in. wide stitched specimens was greatest along the centerlines of the specimens, between the stitches, and surface ply delamination was even more prevalent than in unstitched 3.0-in. specimens. In both sets of unstitched specimens, damage tended to be more localized around the fastener hole than is seen in the stitched specimens. However, it is worth noting that some of the unstitched specimens displayed delamination that exceeded that shown by all of the stitched specimens. Specimen #6 in Figure A1(a) is an example of near total delamination during failure.

Filled hole compression test results are shown in Table 3. The presence of stitches increased the average strength of the FHC specimens slightly, though the increase was less than 1σ. However, the scatter in compressive strength decreased by nearly half in the stitched specimens. The majority of specimens in both sets failed above or below the hole, though always adjacent to either the edge of the hole or the edge of a washer. Fractures generally propagated straight across the gage section and at an angle through the specimen thickness. The stitched specimens show a greater degree of delamination damage directly adjacent to the fastener and the delamination appears to be concentrated between the lines of stitches. The overall degree of damage in the FHC specimens was far lower than that seen in the FHT specimens, as seen in Figure A3. Delamination was far more localized in FHC specimens compared to the FHT specimens, and the presence of stitching appeared to affect the failure mode to a lesser degree. Specifically, in comparing the edge views of the specimens on the left side of Figure A3, the number and extent of delaminations appear similar between the stitched and unstitched specimens. It is worth noting, however, that the unstitched specimens at the top of the figure display a larger residual crack opening than do the stitched specimens at the bottom. A general summary of observations regarding failure modes of the FHC coupons can be found in Tables A2 and A3.

Specimen level data of the inplane shear testing are presented in Tables 4 and 5. Table 6 summarizes the effects of specimen thickness and stitch line placement on shear properties. Examining first the effects of specimen thickness, the specimens with stitching around the notch displayed no significant change in shear modulus and a 4% increase in shear strength when specimen thickness increased from 0.167 in. to 0.223 in. However, the amount of variability in both properties doubled in the thicker specimens. Within the specimen sets with stitching through the root of the notch, Specimen #6 in the 0.233-in. thick specimen set was stiffer than the rest of the specimens in that set and it

failed at a load 32% lower than the weakest of the remaining five specimens. If one declares specimen number 6 to be an outlier then increasing the specimen thickness reduced shear modulus by approximately 6% and increased shear strength less than 1.5%. Considering the effect of stitch placement on shear properties, placement of stitches through the notch reduced shear modulus by approximately 7% in the 0.167-in. specimens and by 13% (>3σ) in the 0.223-in. specimens, compared to specimens of the same thickness and stitching spanning the notch. Shear strength increased by approximately 5% and 4% in the 0.167-in. and 0.223-in. specimens, respectively, in through-stitched specimen set, compared to the sets with stitching spanning the notch.

Photographs of the VNS specimens after testing are provided in Figures A4 and A5. In general, the thicker (0.223-in.) specimens displayed larger residual crack opening displacements than did the thinner (0.167-in.) specimens. In the thinner specimens, the delaminated surface plies remained intact. The surface plies of the thicker specimens, however, tended to split at approximately 0.10-in. intervals during testing. The clearest illustration of this can be found in Figure A4(b) in the top-right and bottom-left specimens. Note the circular marks on the top-right specimen (#6), which indicate slippage and rotation of the specimen in the grips. The strength and modulus of that specimen (Table 4(b)) do not appear to be out of the range of variation seen in the other specimens, indicating that specimen movement occurred late in the test. Of the VNS specimens that were stitched around the notch, four of the six 0.167-in. specimens displayed delamination damage biased toward the side with normal-direction stitches. One specimen had a broken normal-direction stitch, and surface ply delaminations in that specimen propagated past the stitch line. Delaminations in the 'stitched-around' 0.223-in. thick specimens were not biased in either direction; half of the specimen set failed on either side of the notch. Four of the six 0.223-in. specimens had broken stitches and delaminations past a stitch line. In contrast to the 'stitched-around' specimens, delamination in the 'stitched-through' specimens behaved differently. The failure of the 0.167-in thick 'stitched-through' specimens initiated in the central (normal-direction) stitch line and propagated away from the other stitch line, with the delaminations terminating at the grips. One specimen displayed a broken stitch in the central stitch line. Of the six 0.223-in thick 'stitched-through' specimens, all showed signs of failure initiation in the notch root, along that central stitch line. However, four of the specimens delaminated in the direction of the inclined stitches. All four of those specimens had broken stitches in the central stitch line. Delamination in specimens with no broken stitches propagated away from the inclined stitch line.

Concluding Remarks

Notched and un-notched properties were characterized of a carbon fiber textile / epoxy composite material system. Filled-hole tension, filled-hole compression, and V-notch rail shear tests were performed. The effect of specimen width on FHT strength was evaluated by testing specimens whose width and hole diameter were scaled by a factor of two. The effect of stitching on FHT strength was assessed by testing specimens with and without stitching. Filled-hole compression specimens were only tested in one width, but included specimens with and without stitching. The effects of stitching on inplane shear strength were evaluated by testing shear specimens with the stitches placed directly through the root of the specimen notched, and by testing specimen with the double stitch line spanning the notch

Increasing specimen width of the FHT specimens led to a decrease in FHT strength of both stitched and unstitched specimens. However, the presence of unexpectedly large bolt hole clearance in the 3.0-in. specimens casts some doubt on those results. The stitching significantly changed the failure modes of the FHT specimens by constraining propagation of delaminations. The presence of stitching had no effect on FHC strength, but it decreased the variability in that property by half. Unlike the FHT specimens, the failure modes of the FHC specimens appeared nearly identical between stitched and unstitched specimen sets. Specimen thickness had little effect on inplane shear strength, but shear modulus was reduced by approximately 5% in the thick specimens. The presence of stitches in the root of the notch of the VNS specimens led to a decrease in shear modulus between 7% and 13%. The stitches increased ultimate shear strength by 4% -5% in specimens of both thicknesses.

References

1. Velicki, Alex and D. Jegley. PRSEUS Development For The Hybrid Wing Body Aircraft. 11th AIAA Aviation Technology, Integration, and Operations (ATIO) Conference; AIAA-2011-7025.

2. Jegley, Dawn C, and A. Velikci. Status of Advanced Stitched Unitized Composite Aircraft Structure. 51st AIAA Aerospace Sciences Meeting; AIAA-2013-0410.
3. Dow, Marvin. and H B. Dexter. Development of Stitched, Braided, and Woven Composite Structures in the Act Program and at Langley Research Center (1985 to 1997) – Summary and Bibliography. NASA TP-97-206234, November 1997, http://ntrs.nasa.gov/?N=123&Ntk=All&Ntt=Dow%2C%20marvin&Ntx=mode matchallpartial
4. 4. Dexter, H. Benson. and B. A. Stein. Advanced Composite Materials for Airframe Structures, Fiber-TEX 1987- First Conference on Advanced Engineering Fibers and Textile Structures for Composites, NASA CP 3001, Part 1, 1988.
5. Jegley, Dawn C. Behavior of Frame-Stiffened Composites Panels With Damage. 54th AIAA/ASME/ASCE/ AHS/ASC Structures, Structural Dynamics, and Materials Conference, April 8-11, 2013, AIAA 2013-1738.

Table 2. FHT strengths for 1.5-in. wide and 3.0-in. wide specimens

(a) 1.5-in. specimen width w/ 0.25-in. hole diameter

Specimen	Unstitched		Stitched	
	Gross Section Strength, ksi	Net Section Strength, ksi	Gross Section Strength, ksi	Net Section Strength, ksi
1	112.1	134.5	125.5	150.7
2	110.4	132.5	118.7	142.4
3	129.9	155.9	129.0	154.8
4	124.3	149.1	125.2	150.2
5	124.1	148.9	121.0	145.2
6	123.9	148.6	110.9	133.1
Average	**120.8**	**144.9**	**122.3**	**146.8**
Standard Deviation	**7.75**	**9.30**	**6.99**	**8.39**
COV†	**6.41%**		**5.72%**	

(b) 3.0-in. specimen width w/ 0.50-in. hole diameter

Specimen	Unstitched		Stitched	
	Gross Section Strength, ksi	Net Section Strength, ksi	Gross Section Strength, ksi	Net Section Strength, ksi
1	101.8	122.1	92.5	111.0
2	--	--	103.8	124.5
3	97.0	116.3	112.6	135.1
4	103.4	124.1	108.0	129.6
5	95.5	114.6	120.9	145.1
6	107.8	129.3	123.8	148.6
Average	**101.1**	**121.3**	**110.3**	**132.3**
Standard Deviation	**4.96**	**5.96**	**11.55**	**13.86**
COV†	**4.91%**		**10.5%**	

†Coefficient of Variation

Table 3. FHC test results, 1.5-in. specimen width, 0.25-in. hole diameter

Specimen	Unstitched		Stitched	
	Gross Section Strength, ksi	Net Section Strength, ksi	Gross Section Strength, ksi	Net Section Strength, ksi
1	67.0	80.4	76.1	91.3
2	67.7	81.3	76.3	91.5
3	86.2	103.4	76.4	91.7
4	73.0	87.6	73.9	88.7
5	67.8	81.4	71.8	86.2
6	65.2	78.2	65.4	78.5
Average	**71.2**	**85.4**	**73.3**	**88.0**
Standard Deviation	**7.80**	**9.36**	**4.25**	**5.10**
COV†	**11.0%**		**5.80%**	

† Coefficient of Variation

Table 4. VNS test results, stitched around root of notch

(a) 0.167-in. laminate thickness

Specimen	Chord Modulus, Msi	Ultimate Strength, ksi
1	2.38	37.9
2	2.44	39.2
3	2.41	37.8
4	2.36	39.0
5	2.38	40.1
6	2.42	38.3
Average	**2.40**	**38.7**
Standard Deviation	**0.03**	**0.91**
COV†	**1.24%**	**2.34%**

(b) 0.223-in. laminate thickness

Specimen	Chord Modulus, Msi	Ultimate Strength, ksi
1	2.54	38.6
2	2.38	40.6
3	2.46	40.2
4	2.37	37.4
5	2.40	43.5
6	2.34	38.9
Average	**2.41**	**39.9**
Standard Deviation	**0.07**	**2.12**
COV†	**3.03%**	**5.31%**

† **Coefficient of variation**

Table 5. VNS test results, stitched through root of notch

(a) 0.167-in. laminate thickness

Specimen	Chord Modulus, Msi	Ultimate Strength, ksi
1	2.32	42.5
2	2.22	41.3
3	2.11	38.4
4	2.20	40.0
5	2.28	41.4
6	2.20	40.7
Average	**2.22**	**40.7**
Standard Deviation	**0.07**	**1.43**
COV†	**3.28%**	**3.50%**

(b) 0.223-in. laminate thickness

Specimen	Chord Modulus, Msi	Ultimate Strength, ksi
1	2.13	39.7
2	2.14	43.6
3	2.11	39.8
4	2.14	42.0
5	1.98	41.3
6	2.46	27.0
Average	**2.16 [2.10]***	**38.9 [41.3]***
Standard Deviation	**0.16 [0.07]***	**6.00 [1.631]***
COV†	**7.44% [3.27%]***	**15.4% [3.95%]***

† Coefficient of variation

* Assuming that specimen #6 is an outlier

Table 6. Summary of effects of specimen thickness and stitch placement of shear properties

(a) Effect of specimen thickness on shear properties †

Stitch Placement	Specimen Thickness, in.	Chord Modulus, Msi	Ultimate Strength, ksi
Stitched Around	**0.167**	--	--
	0.223	0.69%	4.16%
Stitched Through	**0.167**	--	--
	0.223	-5.58%	1.38%

(b) Effect of stitch placement on shear properties *

Stitch Placement	Specimen Thickness, in.	Chord Modulus, Msi	Ultimate Strength, ksi
Stitched Around	**0.167**	--	--
	0.223	--	--
Stitched Through	**0.167**	-7.40%	5.18%
	0.223	-13.17%	3.56%

† Relative to 0.167 in. thickness

* Relative to stitched-around specimens

Specimen #6 in Table 5(b) is declared an outlier.

Appendix

Table A1. Filled-hole specimen bolt and hole dimensions

(a) Filled-hole tensile specimens

Specimen	1.5-in. Specimen Width		3.0-in. Specimen Width	
	Bolt Diameter, in.	Hole Diameter, in.	Bolt Diameter, in.	Hole Diameter, in.
1	0.247	0.250	0.494	0.511
2	0.247	0.250	0.494	0.512
3	0.247	0.249	0.494	0.508
4	0.247	0.248	0.494	0.511
5	0.247	0.251	0.494	0.508
6	0.247	0.249	0.494	0.509
Average diameter	**0.247**	**0.250**	**0.494**	**0.510**
Average clearance	**0.003**		**0.016**	

(b) Filled-hole compression specimens

Specimen	1.5-in. Specimen Width		3.0-in. Specimen Width	
	Bolt Diameter, in.	Hole Diameter, in.	Bolt Diameter, in.	Hole Diameter, in.
1	0.246	0.255	0.494	0.511
2	0.249	0.250	0.494	0.512
3	0.247	0.253	0.494	0.508
4	0.247	0.253	0.494	0.511
5	0.247	0.255	0.494	0.508
6	0.247	0.258	0.494	0.509
Average diameter	**0.247**	**0.254**	**0.494**	**0.510**
Average clearance	**0.007**		**0.016**	

Table A2. Notes on FHT coupon failures, 1.5-in. specimen width

(a) Unstitched specimens

Specimen	Failure Code	Delamination length, in.	Notes
1	AGM	2.0	1
2	AGM	2.2	1
3	AGM	2.2	1
4	AGM	8.0	2
5	AGM	8.0	3
6	AGO	8.0	4

(b) Stitched specimens

Specimen	Failure Code	Delamination length, in.	Notes
1	AGM	7.0	5
2	AGM	4.5	5
3	AGM	6.3	5
4	AGM	6.0	5
5	AGM	6.5	5
6	AGM	5.2	5

Failure Codes and Notes:

AGM Angle plies thru fracture, located in gage section, middle of specimen
AGO Angle plies thru fracture, located in gage section, offset from center
Note 1 Initiated at hole, propagated toward edges
Note 2 Nearly full-length delamination of all plies
Note 3 Delamination greatest along edges near middle of gage length
Note 4 Offset 1.3 in. from edge of hole
Note 5 Initiated at hole, extensive delamination along both edges

Table A3. Notes on FHT coupon failures, 3.0-in. specimen width

(a) Unstitched specimens

Specimen	Failure Code	Delamination length, in.	Notes
1	AGM	3.0	1
2	AGM	2.3	2
3	AGM	2.5	1
4	AGM	4.2	1
5	AGM	3.9	1
6	AGO	6.5	3

(b) Stitched specimens

Specimen	Failure Code	Delamination length, in.	Notes
1	AGM	3.1	4
2	AGM	6.7	4
3	AGM	3.4	4
4	AGM	8.0	4
5	AGM	6.0	2, 5
6	AGO	5.9	5, 6

Failure Codes and Notes:

AGM Angle plies thru fracture, located in gage section, middle of specimen
AGO Angle plies thru fracture, located in gage section, offset from center
Note 1 Nominally uniform delamination around hole
Note 2 Extensive surface ply delamination
Note 3 Centered 2 in. below center of hole
Note 4 Delamination between stitch lines
Note 5 Biased toward one end
Note 6 Surface delaminations propagated 1 in. under grip.

Table A4. Notes on FHC coupon failures

(a) Unstitched specimens

Specimen	Failure Code	Notes
1	LGO	1,2
2	LGF	1
3	LGF	1
4	LGF	2,3
5	LGM	1
6	LGM	1,3

(b) Stitched specimens

Specimen	Failure Code	Notes
1	LGM	1
2	LGO	1,4
3	LGF	3
4	LGF	1,3
5	LGO	1
6	LGO	2

Failure Codes and Notes:

LGM Longitudinal fracture, located in gage section, middle of specimen
LGO Longitudinal fracture, located in gage section, offset from edge of hole
LGF Longitudinal fracture, located in gage section, offset from edge of fastener
Note 1 Angled fracture through thickness
Note 2 Surface ply delamination
Note 3 Brooming at fracture
Note 4 Fracture propagated in 2 directions

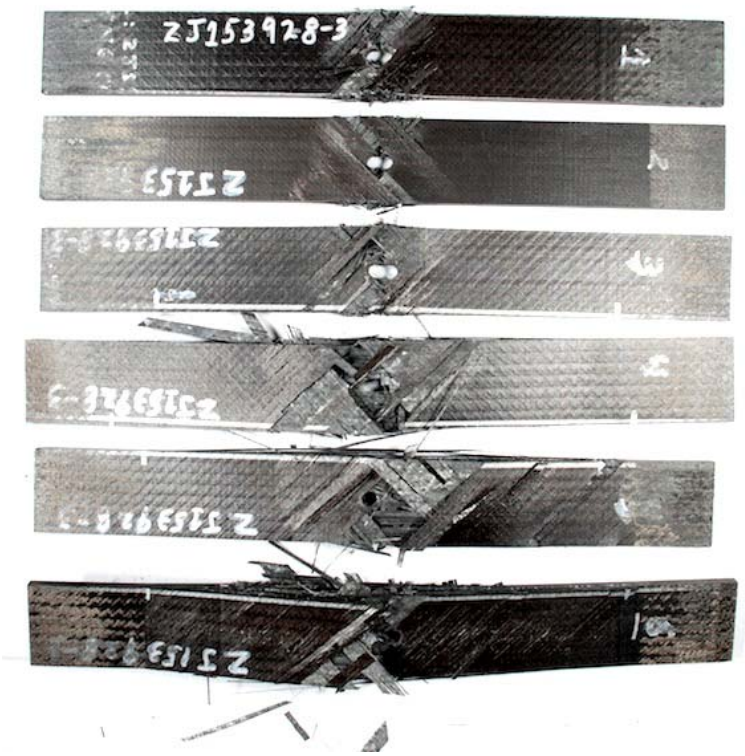

(a) unstitched specimens

(b) stitched specimens

Figure A1. Post-test photographs of FHT, 1.5 in. width

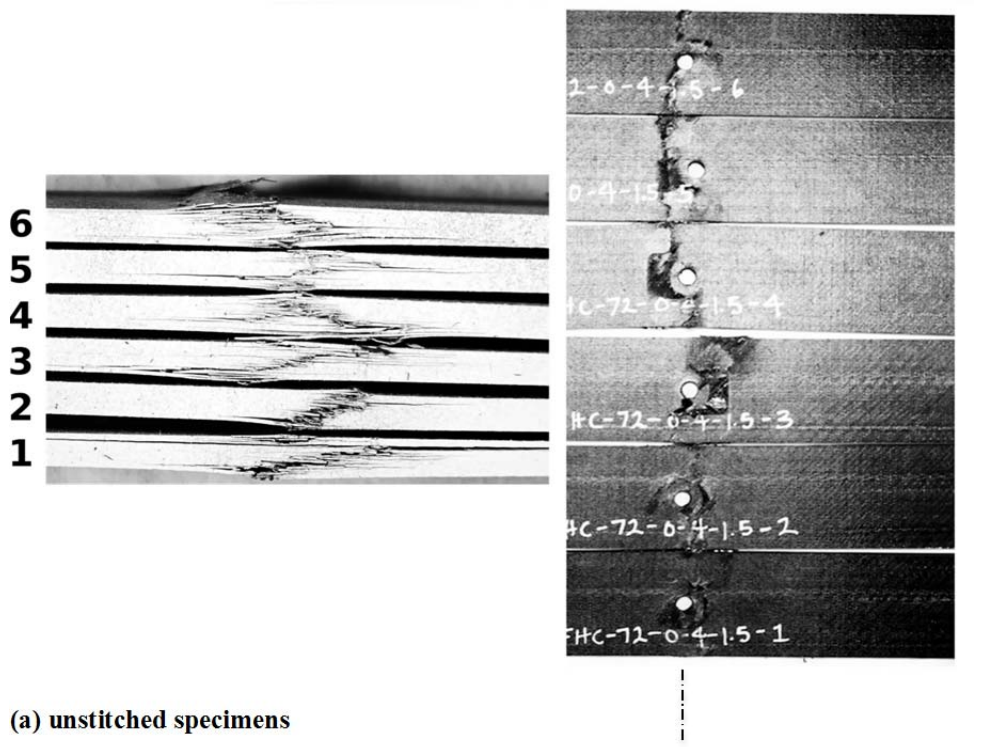

(a) unstitched specimens

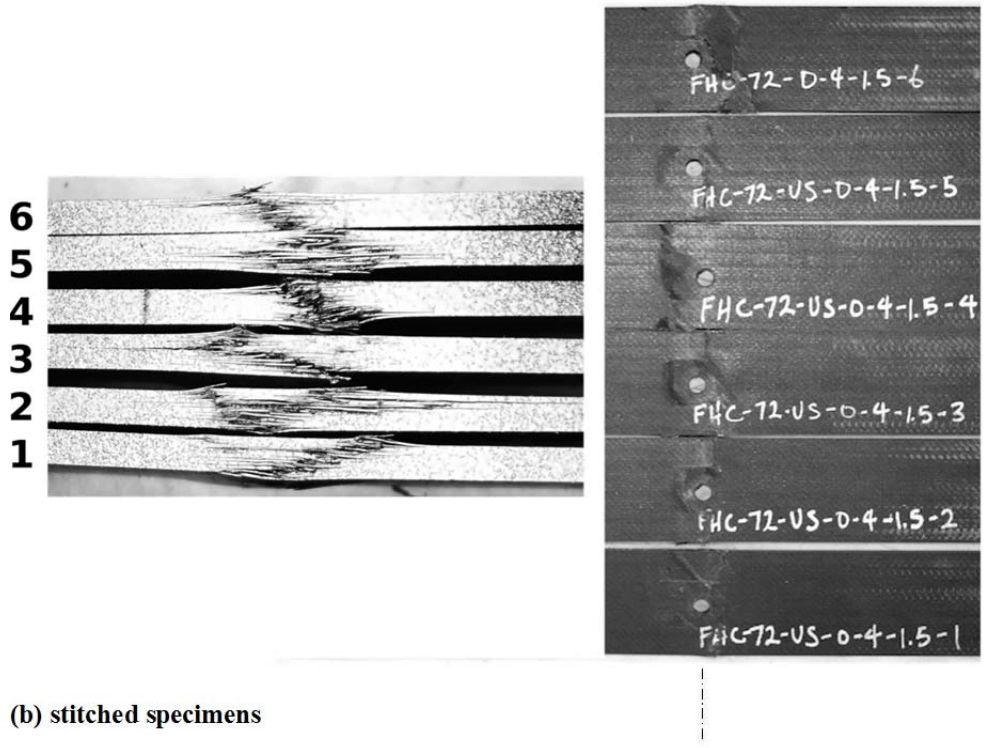

(b) stitched specimens

Figure A3. Post-test photographs of FHC specimens, 1.5 in. width. Face views show right-hand ends of specimens.

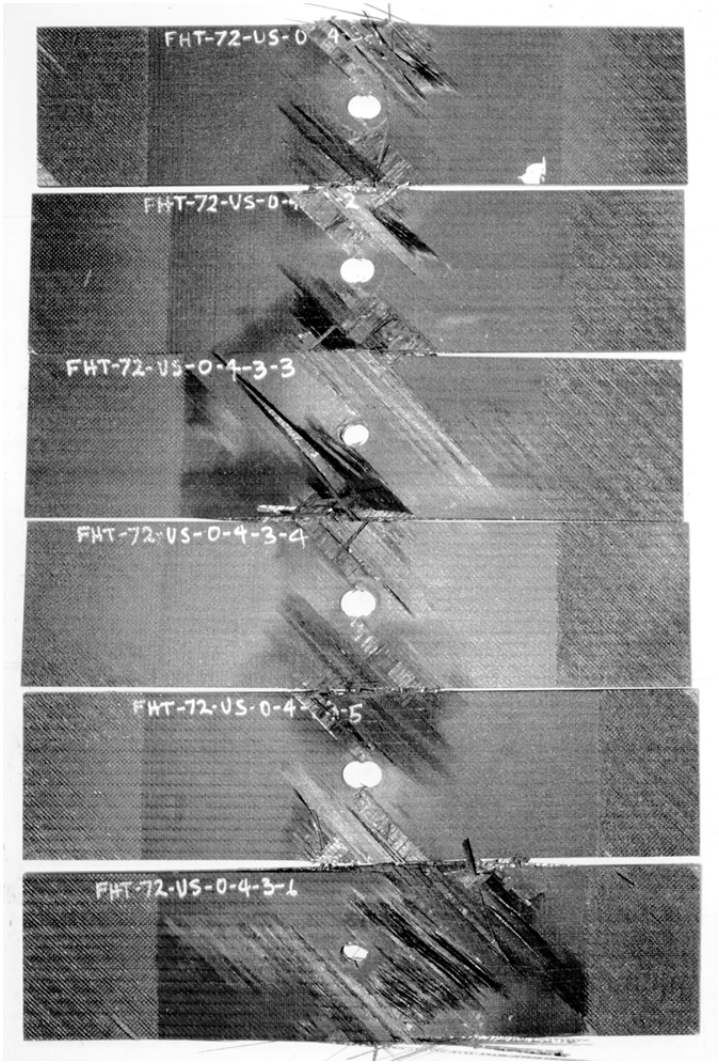

(a) unstitched specimens

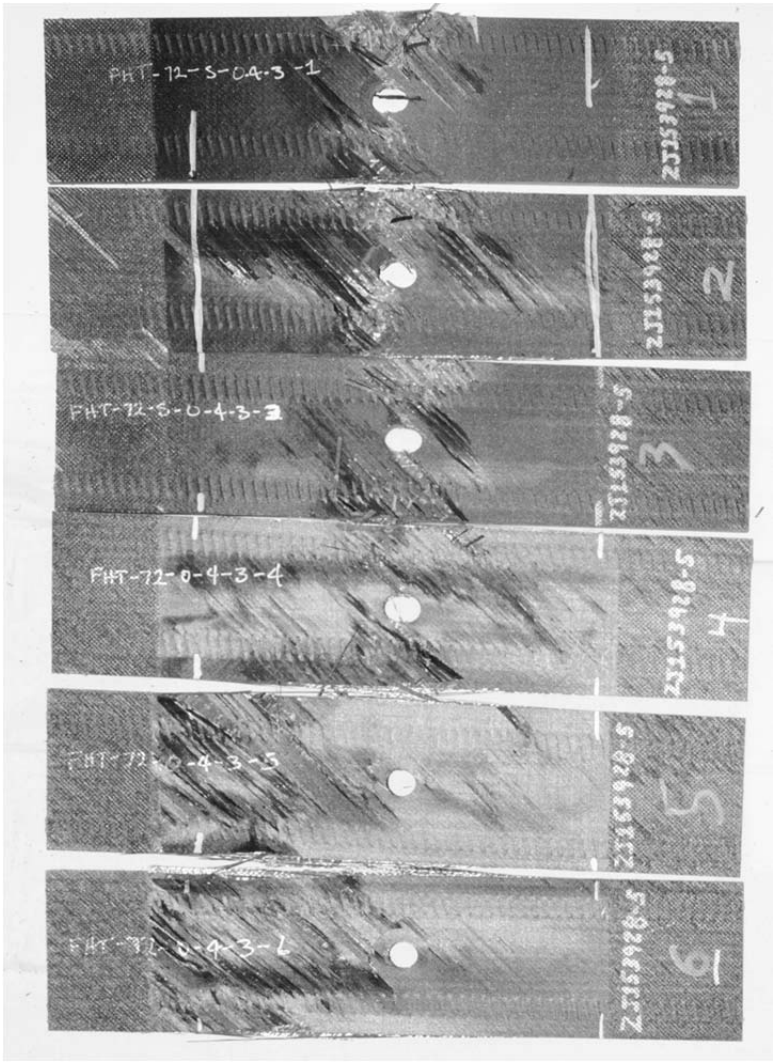

b) stitched specimens

Figure A2. Post-test photographs of FHT specimens, 3.0-in. width

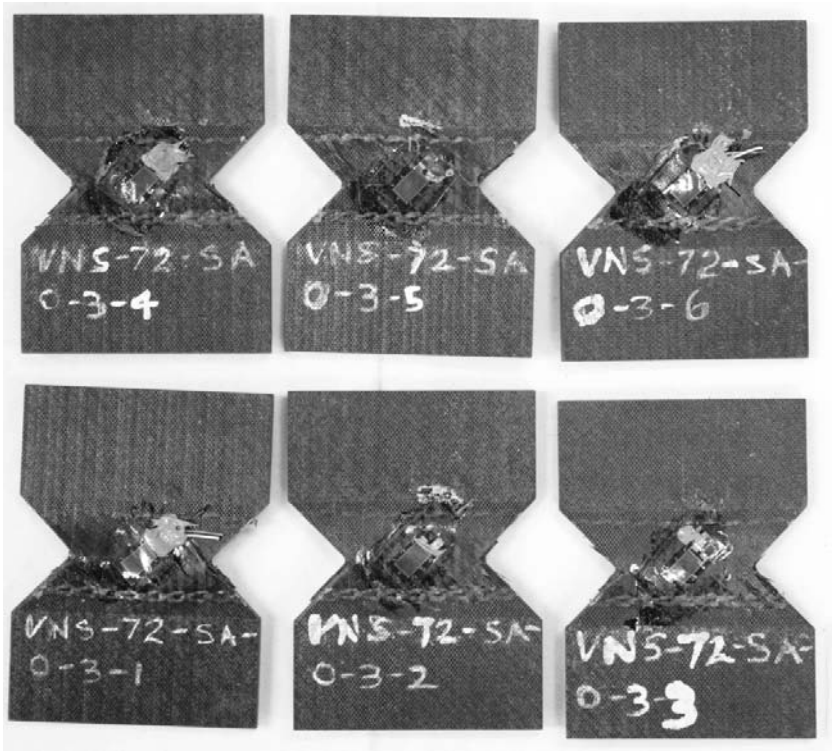

(a) 0.167-in. thickness

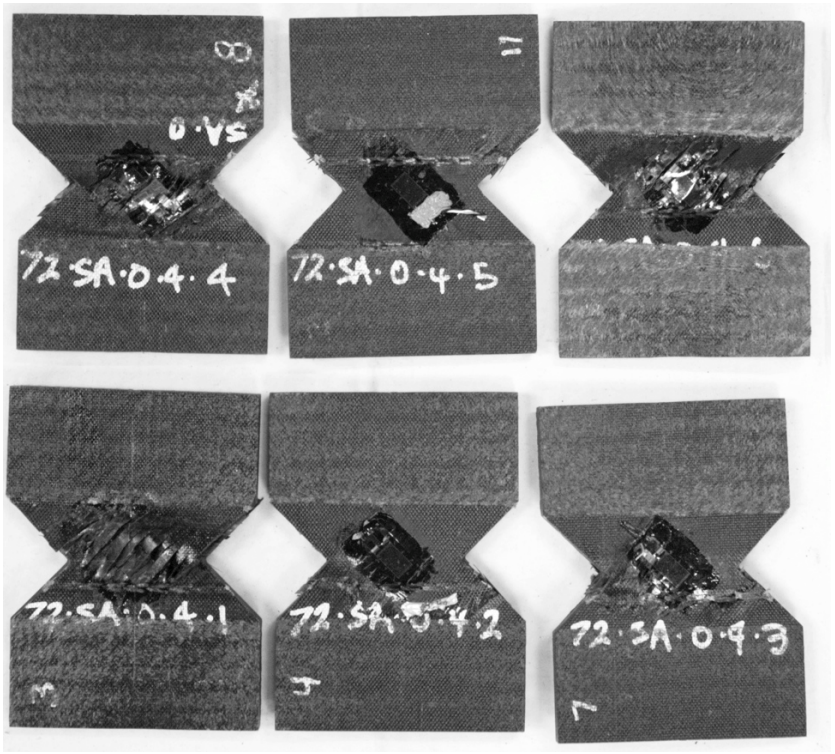

(b) 0.223-in. thickness

Figure A4. Post-test photographs of VNS specimens, stitched around notch

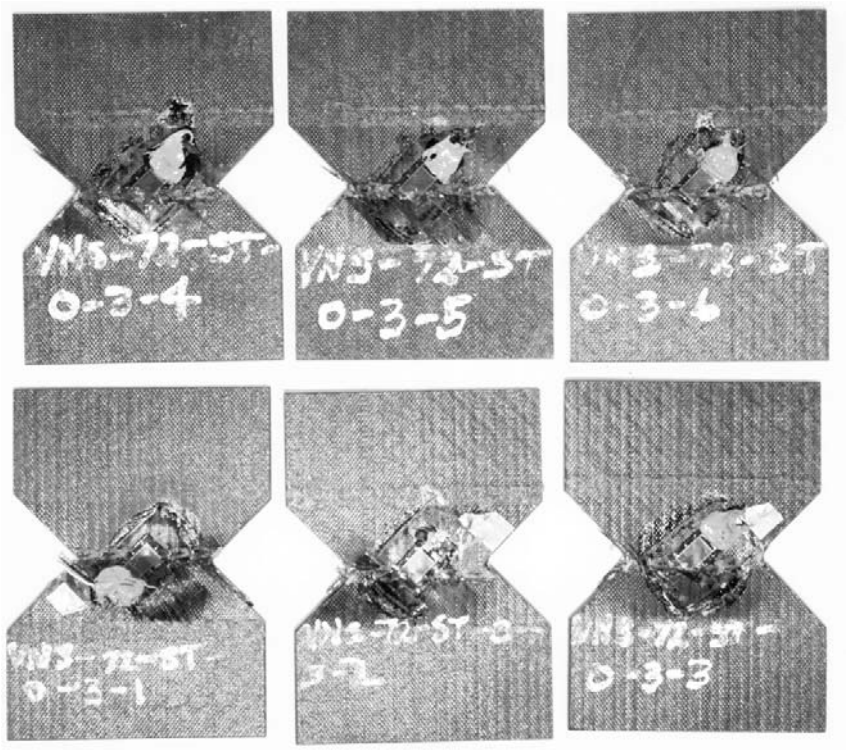

(a) 0.167-in. thickness

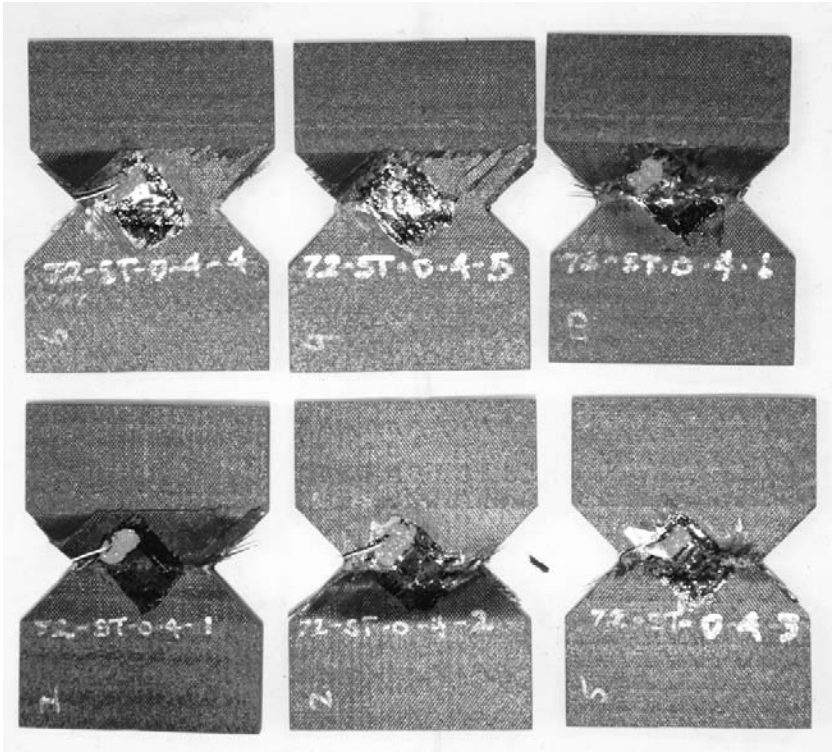

(b) 0.223-in. thickness

Figure A5. Post-test photographs of VNS specimens, stitched through notch

REPORT DOCUMENTATION PAGE

Form Approved
OMB No. 0704-0188

1. REPORT DATE *(DD-MM-YYYY)*	2. REPORT TYPE	3. DATES COVERED *(From - To)*
01- 10 - 2013	Technical Memorandum	

4. TITLE AND SUBTITLE

Notched Strength Allowables and Inplane Shear Strength of AS4/ VRM-34 Textile Laminates

5a. CONTRACT NUMBER

5b. GRANT NUMBER

5c. PROGRAM ELEMENT NUMBER

6. AUTHOR(S)

Grenoble, Ray W.; Johnston, William M.

5d. PROJECT NUMBER

5e. TASK NUMBER

5f. WORK UNIT NUMBER

699959.02.22.07.01.01

7. PERFORMING ORGANIZATION NAME(S) AND ADDRESS(ES)

NASA Langley Research Center
Hampton, VA 23681-2199

8. PERFORMING ORGANIZATION REPORT NUMBER

L-20334

9. SPONSORING/MONITORING AGENCY NAME(S) AND ADDRESS(ES)

National Aeronautics and Space Administration
Washington, DC 20546-0001

10. SPONSOR/MONITOR'S ACRONYM(S)

NASA

11. SPONSOR/MONITOR'S REPORT NUMBER(S)

NASA/TM-2013-218053

12. DISTRIBUTION/AVAILABILITY STATEMENT

Unclassified - Unlimited
Subject Category 01
Availability: NASA CASI (443) 757-5802

13. SUPPLEMENTARY NOTES

14. ABSTRACT

Notched and unnotched strength allowables were developed for a textile composite to provide input data to analytical structural models based on the Pultruded Rod Stiffened Efficient Unitized Structure (PRSEUS) concept. Filled-hole tensile strength, filled-hole compressive strength, and inplane shear strength along stitch lines have been measured. The material system evaluated in this study is based on warp-knitted preforms of AS4 carbon fibers and VRM-34 epoxy resin, which have been processed via resin infusion and oven curing. All specimens were tested in as-fabricated (dry) condition. Filled-hole strengths were evaluated with and without through-thickness stitching. The effects of scaling on filled-hole tensile strength were evaluated by testing specimens in two widths, but with identical width / hole-diameter ratios. Inplane shear specimens were stitched in two configurations, and two specimen thicknesses were tested for each stitch configuration.

15. SUBJECT TERMS

Composites; Hybrid wing body; Out-of-Autoclave; PRSEUS; Stitching; Textiles

16. SECURITY CLASSIFICATION OF:			17. LIMITATION OF ABSTRACT	18. NUMBER OF PAGES	19a. NAME OF RESPONSIBLE PERSON
a. REPORT	b. ABSTRACT	c. THIS PAGE			STI Help Desk (email: help@sti.nasa.gov)
					19b. TELEPHONE NUMBER *(Include area code)*
U	U	U	UU	26	(443) 757-5802